



**Abstract**

Ground deformation in the Azores, at the triple junction between the Eurasian, Nubian, and North American plates, has been mapped with continuous GPS (Global Positioning System) geodetic measurements to improve tectonic motion estimates and for understanding volcanic unrest. We compute daily GPS positions, spanning almost 17 years (2000-2017), from 18 continuous GPS stations. The GPS time-series are analyzed by searching for discontinuities and periodic functions. Results show that Flores and Graciosa islands have displacements close to predicted North American and Eurasian plate motions, respectively, while São Miguel, Terceira, São Jorge, Faial and Pico islands have displacements in between predicted Eurasian and Nubian plate motions. The Eurasian-Nubian plate boundary in the Azores behaves as a diffuse ultra-slow oblique spreading center with focused deformation found in the Central Group and São Miguel Island. The velocity field is modeled by approximating segments of the Eurasian-Nubian plate boundary with vertical dislocations with right-lateral motion and opening below a locking depth. Best fitting models have deep motion in the range of 2.4-2.7 mm yr<sup>-1</sup> directed N(76.5-78.8)°E. Such displacement accounts for more than half predicted Eurasian-Nubian relative plate motion. The modeling results suggest that the locking depth in the Central Group is about 17 km while in São Miguel is about 2 km. We found transient deformation at Fogo volcano, São Miguel Island, due to unrest activity mainly during 2003-2006 and 2011-2012, and local continuous subsidence in Terceira Island, attributed to a deflation source centered on the island.

**Plain Language Summary**

The Azores is located at the junction of three tectonic plates, the North American, Eurasian and Nubian plates. The boundary between the North American and the other two plates is well defined by the Mid-Atlantic Ridge, but the boundary between the Eurasian and Nubian plates is unclear. Ground deformation in the Azores has been mapped with GPS (Global Positioning System) measurements between 2000 and 2017 to estimate tectonic motion and understand volcanic unrest. We calculate the velocity of 18 continuous GPS stations and compare it with predicted velocities from plate motion models. Results show that Flores and Graciosa islands are close to stable North American and Eurasian plate motions, respectively. In contrast, São Miguel, Terceira, São Jorge, Faial and Pico islands are subject to inter-plate motion between the Eurasian and Nubian plates, with focused spreading in the Central Group and São Miguel Island. The velocity field can be explained by the motion of vertical rectangular dislocations in the Central Group and São Miguel Island buried at 17 and 2 km, respectively. The focused spreading in the central part of São Miguel Island helps explain the episodic intrusions at Fogo volcano during unrests.

**1 Introduction**

The Azores archipelago is located at the triple junction between the Eurasian, Nubian, and North American plates (Figure 1). The islands rise from the so-called Azores Plateau, an area of thickened crust, roughly defined by the 2000 m isobath. Estimates of the crustal thickness in the Azores are in the range of 14-17 km (Escartin et al., 2001; Spieker et al., 2018).

The boundary between the North American and the other two plates is well defined by the Mid-Atlantic Ridge (Figure 1), but this is not the case for the boundary between the Eurasian and Nubian plates. The Corvo and Flores islands form the Western Group and are located west of the Mid-Atlantic Ridge, on the North American plate. The other seven islands lie to the east of the Mid-Atlantic Ridge. The Graciosa, Terceira, São Jorge, Faial and Pico islands form the Central Group, while São Miguel and Santa Maria form the Eastern Group.

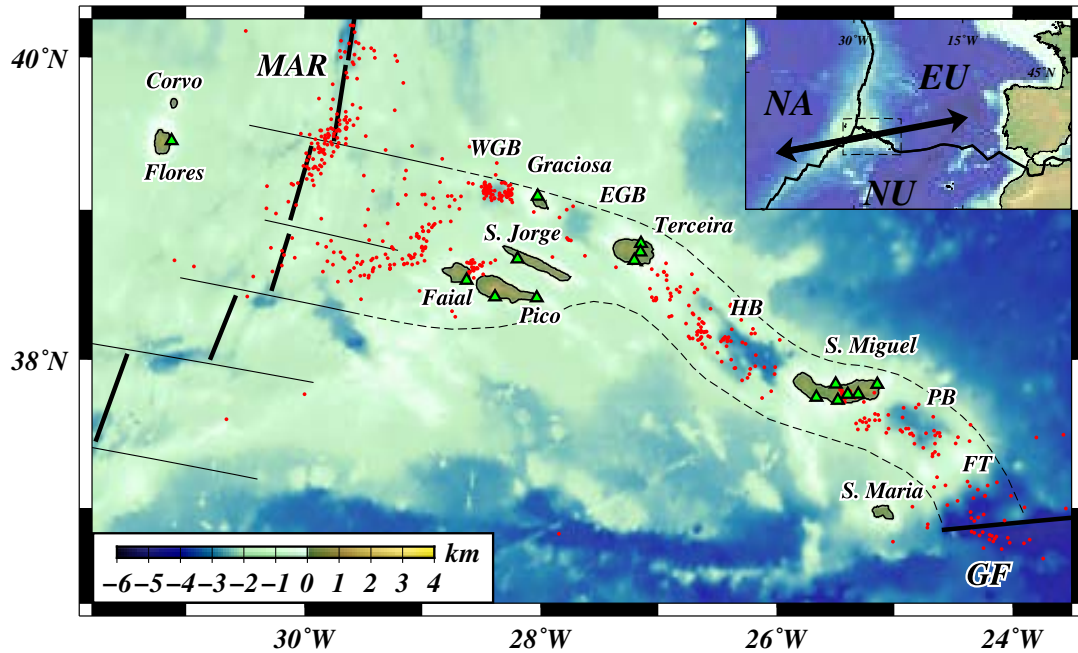


**Figure 1.** Overview of the tectonic setting of the Azores Plateau roughly defined by the 2000 m isobath. Mid-Atlantic Ridge (MAR) segments are represented by heavy black lines and the intersecting fracture zones by black narrow lines (Luis et al., 1994). The Terceira Rift comprises, from west to east, the West Graciosa Basin (WGB), Graciosa Island, East Graciosa Basin (EGB), Terceira Island, Hirondele Basin (HB), São Miguel Island, Povoação Basin (PB) and Formigas Through (FT). The Gloria Fault (GF) is located to the east of Santa Maria Island. The GF and plate boundaries (inset) (DeMets et al., 2010) are represented by black heavy lines. The dashed line represent a proposed area of the Eurasian-Nubian inter-plate deformation zone. Green triangles are continuous GPS stations located in Flores (FLRS), Graciosa (AZGR), São Miguel (PDEL, RIB1, RCHA, PCNG, FRNS, and QBN1, from west to east), Terceira (NOV1, TERC, and SRPC, from north to south), São Jorge (QEMD), Faial (HORT) and Pico (PTRP and PIED, from west to east). Red circles are recorded earthquakes ( $M_L \geq 3$ ) between April 2000 and January 2017 (CIVISA database). The bathymetric and topographic data have been derived from 30 arc seconds resolution SRTM (Becker et al., 2009). The arrows in the inset show the opening rate of  $4.3 \pm 0.1 \text{ mm yr}^{-1}$  in direction  $N(80.5 \pm 2.5)^\circ E$  between EU and NU plates according to ITRF2008 plate motion model (Altamimi et al., 2012), calculated at the average location of all GPS sites to the east of MAR.

70 The so-called Terceira Rift (Machado, 1959; Searle, 1980) is an important geolog-  
 71 ical structure located to the east of the Mid-Atlantic Ridge and comprises a series of basins  
 72 alternating with volcanic highs aligned NW-SE to WNW-ESE direction, from the West  
 73 Graciosa Basin to Formigas Through (Figure 1). To the south of Terceira Rift, the São  
 74 Jorge and Faial-Pico alignments have a general WNW-ESE direction defined by the is-  
 75 lands volcanic systems and adjacent submarine volcanic ridges.

76 Previous GPS (Global Positioning System) geodetic measurements in the Azores  
 77 show that to the east of the Mid-Atlantic Ridge, Graciosa and Santa Maria islands have  
 78 displacements closer to predicted Eurasian and Nubian motion, respectively, while the  
 79 other islands display an intermediate motion (Fernandes et al., 2006). According to plate  
 80 motion models based on geologic and geodetic data (Argus et al., 2010; DeMets et al.,

2010; Altamimi et al., 2012), the predicted plate spreading between the Eurasian and Nubian plates in the Azores is slow compared with most active plate spreading regions, with full velocity in the range of 4.2–4.8 mm yr<sup>-1</sup> and direction of N(73–82)°E. The plate boundary is highly oblique to this direction with a strike ranging N(45–75)°W. This obliquity leads to a complex deformation zone accommodating right-lateral shear and extension.

Since the fifteenth century, many destructive earthquakes and volcanic eruptions have been registered in the Azores (Gaspar et al., 2015). Most seismic activity is located on the Mid-Atlantic Ridge, the Terceira Rift, and on the Faial-Pico alignment towards the Mid-Atlantic Ridge (Figure 1). Some areas are more affected by seismic activity than others. For example, the central area of São Miguel Island, has experienced periods of increased seismic activity (Silva et al., 2012). Ground deformation including inflation and deflation of Fogo volcano was observed in the unrest episodes of 2003–2006 (Trota, 2008) and 2011–2012 (J. Okada et al., 2015).

This study reports results from 18 continuous GPS stations (CGPS) in the Azores from April 2000 to January 2017. The time-series show long-term displacements due to plate motion in the Azores and temporal variations of the deformation, particularly in the central area of São Miguel Island during periods of unrest.

## 2 CGPS and Data Analysis

### 2.1 The CGPS network

CGPS (Continuous GPS) station measurements in the Azores began in 2000 with the installation of the PDEL station in Ponta Delgada, São Miguel Island (Figure 1). In 2002 RIB1 station was installed on São Miguel Island and in 2003 three stations were installed: QBN1 in São Miguel Island and NOV1 and SRPC on Terceira Island. In 2005, HTN1, PCNG, and RCHA stations were installed on São Miguel Island. On the same island, BVF1 was installed in 2007. A regional CGPS network (REPRAA, 2021) was created to support users interested in precise GPS data from the region. Three stations were installed in 2008: AZGR on Graciosa Island, FRNS on São Miguel Island, and TERC on Terceira Island. Other three stations started operating in 2009: FLRS on Flores Island, PIED on Pico Island, and VFDC on São Miguel Island. More recently, PTRP station was installed on Pico Island in 2010, QEMD station on São Jorge Island in 2012, and HORT station on Faial Island in 2013.

Most of the CGPS monuments of CIVISA (Centro de Informação e Vigilância Sismovulcânica dos Açores) consist of a ~1-meter high stainless steel rod screwed in a stainless steel benchmark cemented directly into a solid bedrock or a concrete platform with a deep foundation in soil. The benchmarks are leveled during the installation, and the GPS antennas are fastened to the top of the rod. Choke ring antennas are used with radomes covering most of them. Some stations are located in public buildings, with the antennas fixed at the top, while other stations are remote. Presently, most of the remote stations contain solar panels, batteries, and data transmission devices. However, some stations have been operated without data transmission devices for several years, and data were collected intermittently. This resulted in data gaps in some stations, especially during the first years of observation. The data files from CGPS stations with data transmission are downloaded automatically daily via ADSL or digital radio to the CIVISA database.

Presently, CIVISA together with IVAR (Instituto de Vulcanologia e Avaliação de Riscos), operates a CGPS network comprising around 30 stations, aiming to monitor ground deformation in near real-time and to contribute to a better understanding of processes causing deformation in the Azores.

## 2.2 Data Processing

Dual-frequency phase and pseudo-range data at 30-second intervals are recorded at all CGPS stations in 24 hour-long RINEX files, with antenna elevation angle limit set in the range of 5°-15°, depending on the local terrain and open-sky visibility.

The daily positions of the CGPS stations are calculated using the RINEX files and reprocessed precise orbits from the Center for Orbit Determination in Europe (CODE) aligned to the ITRF2008 reference frame (Susnik et al., 2016). Data from about 50 stations from the International GNSS Service (IGS) are also used. The data is analyzed using Bernese 5.2 software (Dach & Walser, 2015) using the following strategy: (1) pre-processing, including receiver clock synchronization and cycle slip correction; (2) initial ionosphere-free analysis with computation, analysis, and removal of residuals; (3) ambiguity resolution scheme using multiple strategies depending on the length of the baseline: Code-Based Widelane (WL), Phase-Based Widelane (L5), Quasi-Ionosphere-Free (QIF) and Direct L1/L2; (4) computation and analysis of station coordinate solutions and uncertainties. All the daily coordinate solutions are transformed into the ITRF2008 reference frame with a 3-parameter Helmert solution imposed on the coordinates of 20 fiducial stations from the IGS (ALGO, BOR1, BREW, DRAO, DUBO, GODE, GODZ, JOZE, MAR6, MATE, NYAL, ONSA, STJO, THU3, WILL, WSRT, WTZR, YEBE, YELL, and ZIMM). We selected the fiducial stations after checking the data quality from the GPS time-series analysis performed by JPL. The processing utilizes absolute antenna phase center offset models from the IGS (Schmid et al., 2016), ocean tidal loading effects from FES2004 model (Lyard et al., 2006), troposphere refraction effects from Vienna Mapping Function data (Böhm et al., 2006), and zenith path delay corrections from the European Centre for Medium-Range Weather Forecasts.

## 2.3 Time-series and Velocity Estimation

### 2.3.1 Time-series Analysis

The coordinate time-series resulting from data processing, in the ITRF2008 reference frame, are evaluated using the FODITS program included in the Bernese 5.2 software. FODITS allows computing functions that fit times-series. The functions include four elements: outliers, discontinuities, linear velocities, and periodic functions. A statistical test, based on the defined user level of significance, terminates the analysis when the model adequately represents the time-series (Dach & Walser, 2015).

The discontinuities in GPS time-series are the result of equipment changes or ground deformation processes. Known equipment changes at the CGPS stations (see Table S1) are detected as discontinuities in the time-series using FODITS (see Table S2).

In addition to discontinuities from known equipment changes, there are others of unknown origin (see Table S2). These discontinuities may relate to unreported equipment changes or ground deformation processes. It was not possible to check equipment changes in some cases, especially from older data-sets and from the REPRAA agency stations. We find unknown discontinuities in the time-series of AZGR, PDEL, and SRPC stations located in relatively stable areas where no significant seismic activity was recorded. These discontinuities are very sudden and classified as unreported equipment changes. Additional unknown discontinuities are found in the time-series of stations located around the Fogo volcano. These discontinuities happen more gradually during the 2003-2006 and 2011-2012 unrest periods of Fogo, and are classified as ground deformation events.

The amplitudes of the seasonal signals found in the time-series (see Table S3) are small when compared with values found, for example, at CGPS stations in Iceland where water and snow loading effects are large (Geirsson et al., 2006; Drouin et al., 2016). Amplitudes of seasonal signals estimated in this study are in the range of 0.8-2.5 mm in the

**Table 1.** Velocities of the more stable CGPS stations in the ITRF2008 reference frame, with  $1\sigma$  Uncertainties, in East, North, and Up components, and correlation factor between horizontal components

Station	Latitude	Longitude	Date Interval	Velocity (mm yr <sup>-1</sup> )			Corr
				E	N	U	
<i>AZGR</i>	39.088	-28.023	2008/07 - 2016/07	15.1 ± 0.3	16.7 ± 0.3	-2.7 ± 0.6	-0.1
<i>FLRS</i>	39.454	-31.126	2009/01 - 2017/01	-9.9 ± 0.6	20.1 ± 0.3	-1.3 ± 1.1	-0.2
<i>FRNS</i>	37.769	-25.308	2008/07 - 2016/07	14.9 ± 0.4	15.9 ± 0.5	-1.2 ± 1.0	-0.1
<i>HORT</i>	38.531	-28.626	2013/03 - 2016/03	12.1 ± 0.9	15.4 ± 0.9	-4.1 ± 2.1	-0.2
<i>HTN1</i>	37.773	-25.315	2005/05 - 2012/05	15.0 ± 0.4	15.7 ± 0.6	-1.1 ± 1.3	-0.1
<i>NOV1</i>	38.776	-27.149	2003/02 - 2016/02	13.3 ± 0.2	15.1 ± 0.2	-2.8 ± 0.5	-0.1
<i>PDEL</i>	37.748	-25.663	2000/05 - 2016/05	12.6 ± 0.2	16.1 ± 0.2	-1.6 ± 0.4	-0.1
<i>PIED</i>	38.414	-28.032	2009/01 - 2017/01	11.8 ± 0.3	14.9 ± 0.4	-2.3 ± 0.7	0.0
<i>PTRP</i>	38.420	-28.386	2010/05 - 2016/05	11.8 ± 0.5	15.6 ± 0.6	-3.0 ± 1.4	-0.1
<i>QBN1</i>	37.835	-25.146	2003/07 - 2016/07	14.8 ± 0.2	16.9 ± 0.2	-1.0 ± 0.5	0.1
<i>QEMD</i>	38.672	-28.194	2012/11 - 2016/11	12.7 ± 0.5	15.6 ± 0.6	-1.9 ± 1.4	0.0
<i>SRPC</i>	38.663	-27.205	2003/02 - 2016/02	13.9 ± 0.2	16.8 ± 0.2	-3.5 ± 0.5	0.0
<i>TERC</i>	38.719	-27.153	2008/09 - 2016/09	12.8 ± 0.3	16.3 ± 0.4	-3.8 ± 0.7	-0.1

179 horizontal components and 0.4-3.7 in the vertical component. The seasonal signals are  
180 more clear in the north component than in the east and up components, ranging in the  
181 direction from 151° to 173° at most stations. It was not possible to estimate seasonal  
182 signals for the time-series of HORT and QEMD stations because of the short period of  
183 observations.

184 Using the results of FODITS, we remove outliers, discontinuities from equipment  
185 changes, and annual seasonal signals from the time-series in the ITRF2008 reference frame  
186 (Figure S1). Other discontinuities are not removed from the time-series.

### 187 2.3.2 Velocity Estimation

188 We estimate the time-series velocities in the ITRF2008 reference frame using lin-  
189 ear fitting of the data (Table 1). Similarly to Geirsson et al. (2006), we estimate the ve-  
190 locity uncertainty from the variance of the residuals of the regression and the length of  
191 the time-series, using the formula  $\sigma_v = \sigma/T$ , where  $\sigma$  is the standard deviation of the  
192 residuals and T is the length of the time series in years. A correlation factor between the  
193 horizontal velocity error components is computed from the covariance of the residuals.  
194 The velocities of stations at Fogo volcano are not estimated because of the transient dis-  
195 turbances in the time-series.

196 We finally remove the ITRF2008 predicted motion (Altamimi et al., 2012) from the  
197 estimated time-series velocities (Figures 2C, 3C and S2). The time-series of FLRS sta-  
198 tion is relative to predicted North American plate motion, while all other time-series are  
199 relative to predicted Eurasian plate motion. There are differences in the time-span of  
200 the time-series of the CGPS stations. The station with the longest time-series is PDEL  
201 spanning almost 17 years, whereas the station with shortest time-series is HORT with  
202 almost 4 years. There are some gaps in the time-series, mostly at remote stations op-  
203 erating without data transmission devices. The time-series from PDEL, HTN1, FRNS,  
204 and QBN1 stations at São Miguel Island and the stations at the other islands show sta-  
205 ble displacements. In contrast, the time-series of RIB1, RCHA, BVF1, VFDC, and PCNG  
206 stations located at Fogo volcano, in São Miguel Island, show significant variations in the

rate of the displacement, as a result of unrest episodes at the volcano during the study period.

### 3 Eurasian-Nubian Plate Spreading

#### 3.1 Velocity Field and Predicted Motion

We analyze the regional deformation field in more detail from the estimated velocities of the more stable CGPS stations. We exclude the data from the stations located around Fogo volcano affected by transient deformation. Most previous ground deformation studies have relied on sparse GPS data, mostly from annual campaign surveys (Fernandes et al., 2006; Trota et al., 2006; Miranda et al., 2012; Marques et al., 2013; Mendes et al., 2013). Besides lower temporal resolution, the data from campaign observations have several limitations, such as high susceptibility to severe atmospheric conditions, multipath error, and bad satellite geometry, resulting in lower precision of the estimated velocities. The number of stations used in this study is small compared with some previous GPS campaign surveys, but the higher temporal resolution of the CGPS data allows estimating velocities with higher precision. Therefore, CGPS data analyses allow us to better discriminate between long-term displacements such as plate motion and local short-term displacements such as volcano deformation.

The velocities show differential motion between the CGPS stations (Table 1). In the ITRF2008 reference frame, the FLRS station on the North American plate is moving at a rate of  $22.4 \text{ mm yr}^{-1}$  in direction  $\text{N}26^\circ\text{W}$ . In contrast, all other stations located east of the Mid-Atlantic Ridge are moving at a rate of  $20.5^{+1.9}_{-1.6} \text{ mm yr}^{-1}$  to  $\text{N}(39^{+4}_{-2})^\circ\text{E}$  in the same reference frame.

Various plate motion models provide estimates of plate spreading direction and full plate velocity across the Azores. We use the ITRF2008 plate motion model (Altamimi et al., 2012), which has an intermediate Eurasian-Nubian full plate velocity compared with MORVEL2010 (DeMets et al., 2010) and GEODVEL2010 (Argus et al., 2010) (see Table S4). We compare the horizontal velocity of FLRS station with predicted stable North American displacement and the velocities of the stations located in the Central Group and São Miguel Island with both the predicted stable Eurasian and Nubian velocities.

The station on Flores Island (FLRS) (Figure 4A) moves with a velocity close to predicted North American velocity and the lack of significant recorded seismic activity in the area is an indication that the island is located on a relatively stable area. However, the deviation of  $\sim 3 \text{ mm yr}^{-1}$  between estimated and predicted motion suggests that the island could be subject to local deformation. Using the GEODVEL2010 and MORVEL2010 plate motion models we get a slightly better correlation between estimated and predicted velocities. The deviation may also relate to the lack of data from this area in the eastern edge of the North American plate used to compute plate motion models.

The station located on Graciosa Island (AZGR) (Figure 4B) moves close to predicted Eurasian motion. The maximum estimated Eurasian-Nubian motion is found between this station and PIED station located on the eastern part of Pico Island. The AZGR station is moving at a rate of  $3.7 \pm 0.2 \text{ mm yr}^{-1}$  to  $\text{N}(62 \pm 4)^\circ\text{E}$  relative to PIED station, which is  $\sim 85\%$  of predicted spreading in the area, indicating that the inter-plate deformation zone is broader than the area between the two stations. Despite the displacement close to Eurasian predicted motion, the recurrent seismicity west of Graciosa is an indication that the island is located in an active deformation area.

The stations located in the eastern part of São Miguel Island (HTN1, FRNS, and QBN1) (Figure 4C) and Terceira Island (NOV1, TERC, and SRPC) (Figure 4D) are also moving close to predicted Eurasian motion, but at a lower rate. The small deviation of

256 the QBN1 velocity is an indication that the eastern part of São Miguel Island is not fully  
 257 within the predicted stable Eurasian plate and is subject to some inter-plate deforma-  
 258 tion.

259 On the other hand, PDEL station on the western part of São Miguel Island and  
 260 the stations located on São Jorge (Figure 4E), Faial (Figure 4F) and Pico (Figure 4G)  
 261 islands have higher displacements away from the Eurasian predicted motion and displace-  
 262 ments closer to the Nubian motion. Spreading between the western and eastern parts  
 263 of São Miguel Island is revealed from the differential motion between PDEL station and  
 264 stations HTN1, FRNS and QBN1, with a maximum displacement of  $2.4 \pm 0.2 \text{ mm yr}^{-1}$   
 265 in direction  $N(72 \pm 2)^\circ E$  and  $0.17 \mu\text{strain}$ . The station QEMD on São Jorge Island is  
 266 moving closer to the Eurasian motion than the stations on Faial and Pico islands. The  
 267 station PIED in the eastern part of Pico Island has the fastest displacement away from  
 268 Eurasian motion and closer to Nubian motion. The other stations, HORT on Faial and  
 269 PTRP on Pico, are moving with intermediate displacements relative to QEMD and PIED  
 270 stations. The similar velocities displayed from HORT and PTRP stations located on Fa-  
 271 ial and Pico islands, respectively, suggest that the eastern part of Faial Island and the  
 272 western part of Pico Island are moving as a block as indicated from previous campaign  
 273 GPS surveys (Marques et al., 2013). Both HORT and PTRP stations move about  $1 \text{ mm}$   
 274  $\text{yr}^{-1}$  away from QEMD station located on São Jorge Island. The small differential mo-  
 275 tion observed between the stations of São Jorge and Faial/Pico islands constitute evi-  
 276 dence that spreading occurs between the islands.

277 Comparing with previous GPS studies in the Azores, the values of the vertical ve-  
 278 locities in this study are well constrained, with uncertainties ranging from sub-millimeter  
 279 level to a few millimeters. The results from the more stable CGPS stations show that  
 280 the Azores Islands are subsiding at an average rate of  $2.3 \pm 0.4 \text{ mm yr}^{-1}$  during the study  
 281 period (see Table 1).

### 282 3.2 Plate Boundary Modeling

283 Previous studies of geodetic measurements across oblique spreading plate bound-  
 284 ary such as the Reykjanes Peninsula, southwest Iceland (Árnadóttir et al., 2006; Keid-  
 285 ing et al., 2008) have used analytical models of opening and shearing dislocation sources  
 286 to fit observed horizontal velocity fields. We follow this approach and approximate seg-  
 287 ments of the Eurasian-Nubian plate boundary with infinitely long-buried vertical rect-  
 288 angular dislocations, embedded within uniform elastic half-space (Y. Okada, 1985). We  
 289 perform the modeling for the Central Group (Figure 5A) and São Miguel Island (Fig-  
 290 ure 5B) in separate runs using different dislocations. We assume that the dislocations  
 291 have opening and right-lateral slip displacements. The dislocations have a locking depth,  
 292 which represents the depth of the brittle-ductile boundary in the crust. The brittle crust  
 293 is locked while the ductile part below opens and slips freely.

294 We perform an inversion of the data to estimate the best fit values of the locking  
 295 depth, opening and right-lateral slip by determining the minimum value of the chi-square  
 296 statistic between observed velocities of the CGPS sites and model predictions (Table 2),  
 297 using the Dmodels software (Battaglia et al., 2013).

298 Before the inversion, we corrected the velocity field from a local subsidence in Ter-  
 299 ceira Island by estimating the deformation generated by a spherical source of pressure  
 300 decrease within uniform elastic half-space (Mogi, 1958) located between Guilherme Mo-  
 301 niz caldera and Pico Alto volcano summit at 5 km depth, with a volume change of  $-2.5 \times$   
 302  $10^5 \text{ m}^3 \text{ yr}^{-1}$ . During the inversion, we search for a locking depth in the range of 1-20 km,  
 303 following estimates of crustal thickness in the Azores. The opening and slip motion vari-  
 304 ables are constrained between zero (no displacement) and the maximum predicted Eurasian-  
 305 Nubian relative plate motion of  $4.8 \text{ mm yr}^{-1}$  (see Table S4).

**Table 2.** Elastic Half-space Dislocation Model Parameter Estimates for São Miguel Island (SM) and Central Group (CG)

Model	Stations	Depth (km)	Velocity (mm yr <sup>-1</sup> )			Azimuth <sup>b</sup> (N°E)	$\chi^2_\nu$
			Open	Slip	Deep Motion <sup>a</sup>		
SM1	4	1.8	1.6	2.2	2.7	76.5	1.1
CG1	8	17.4	1.3	2.0	2.4	78.8	2.9
CG2	8	20.0	1.8	2.4	3.0	76.7	2.6

<sup>a</sup>Magnitude of the vector sum of the right-lateral slip and opening.

<sup>b</sup>Direction of the deep motion.

306 We use geologic, geodetic and seismic data to constrain the location and direction  
 307 of the dislocations. Neotectonic studies show that the dominant morpho-tectonic struc-  
 308 tures at São Miguel Island are NW-SE to WNW-ESE trending faults (Carmo et al., 2014;  
 309 Madeira et al., 2015). The location of the boundary in the central part of São Miguel  
 310 Island, between Fogo and Furnas volcanoes, is constrained from previous geodetic and  
 311 seismic studies (Jónsson et al., 1999; Trota et al., 2006; Silva et al., 2012; J. Okada et  
 312 al., 2015). We test a dislocation model with the N112.5°E direction (WNW-ESE) and  
 313 assume it crosses the seismically active Achada das Furnas fissure zone between Fogo and  
 314 Furnas volcanoes, where the main morpho-tectonic structures have a WNW-ESE direc-  
 315 tion (see Figure 3A). There is more uncertainty about the location of the spreading axis  
 316 in the Central Group. There we test the dislocation model with two different locations  
 317 (see Figure 2A): between Faial-Pico islands and São Jorge Island (CG1), and between  
 318 Graciosa-Terceira islands and São Jorge Island (CG2). We also define the dislocation ori-  
 319 entation in the Central Group as N112.5°E following the main orientation of the shape  
 320 of the islands and surrounding bathymetric structures (Lourenço et al., 1998).

321 The model results (Table 2) for São Miguel Island (SM1) predicts a deep motion  
 322 of 2.7 mm yr<sup>-1</sup> in N76.5°E direction, with 1.6 mm yr<sup>-1</sup> opening motion, and 2.2 mm yr<sup>-1</sup>  
 323 right-lateral slip motion. The locking depth is about 2 km, much shallower than the crustal  
 324 thickness in the Azores. It may be an underestimate because of the relatively low num-  
 325 ber of CGPS stations from São Miguel Island used in the modeling. For the Central Group,  
 326 we favor the model CG1 over CG2, despite the slightly higher chi-square value. The qual-  
 327 ity of fit in the stations located on Terceira Island is similar in the CG1 and CG2 mod-  
 328 els. On the other hand, the quality of fit in the stations located on São Jorge, Faial and  
 329 Pico islands is better in the CG1 model, while the quality of fit in the AZGR station lo-  
 330 cated on Graciosa Island is better in the CG2 model. The CG1 model predicts a deep  
 331 motion of 2.4 mm yr<sup>-1</sup> at N78.8°E direction, with 1.3 mm yr<sup>-1</sup> opening motion, and 2.0  
 332 mm yr<sup>-1</sup> right-lateral slip motion. The locking depth is about 17 km, agreeing well with  
 333 estimates of crustal thickness.

#### 334 4 Seismic Activity and Volcano Deformation

335 Some areas in the Central Group are more affected by seismic activity than oth-  
 336 ers, including the northeast area of Faial Island (see Figure 2). Many earthquakes north-  
 337 east of Faial Island are clustered at deep levels, between 10 and 20 km (see Figure 2B).  
 338 Most seismic activity in this area occurred before 2007 and is possibly related in part  
 339 to crustal relaxation processes after the 1998 major earthquake ( $M_L$  5.8) that occurred  
 340 in the area (Matias et al., 2007). The station HORT located about 10 km south of the  
 341 area most affected by seismicity in Faial Island was installed in 2013. The time-series  
 342 of this station show no transient disturbances.

343 The central part of Terceira island is also affected by higher seismic activity. We  
 344 find relatively high subsidence levels in the stations located on Terceira island, with a  
 345 maximum estimated subsidence rate of  $3.8 \pm 1.0 \text{ mm yr}^{-1}$  at TERC station located close  
 346 to the center of the island. Also, the horizontal velocities of Terceira stations show con-  
 347 vergence towards the center of the island.

348 The central part of São Miguel Island has been the stage of recurrent unrest ac-  
 349 tivity in the last 20 years. The seismic activity is mainly concentrated in the central area  
 350 of São Miguel Island, between Fogo and Furnas volcanoes, and is characterized by a large  
 351 number of small magnitude events along the main fault system. Most seismic events in  
 352 the area have hypocenters above the 5 km depth level (see Figure 3B). There were sev-  
 353 eral episodes of unrest activity in the central part of São Miguel Island during the study  
 354 period, including a major episode in 2005 with a maximum of more than 150 events ( $M_C$   
 355  $\geq 2$ ) recorded per month. Evidence of volcano deformation at Fogo, with both inflation  
 356 and deflation, is inferred from the time-series of stations RIB1, RCHA, BVF1, VFDC,  
 357 and PCNG located around the volcano (see Figure 3C).

## 358 5 Discussion

359 Our results show that Flores Island has a very distinct motion compared with the  
 360 other islands consistent with its location in the North American plate. Graciosa Island  
 361 shows a displacement close to predicted Eurasian motion, while São Miguel, Terceira,  
 362 São Jorge, Faial and Pico islands have displacements in between predicted Eurasian and  
 363 Nubian motions. The modeling results predict a deep motion of  $2.7 \text{ mm yr}^{-1}$  at  $N76.5^\circ E$   
 364 direction for São Miguel Island, and  $2.4 \text{ mm yr}^{-1}$  at  $N78.8^\circ E$  direction for the Central  
 365 Group. This motion account for 50-64% of predicted Eurasian-Nubian relative plate mo-  
 366 tion.

367 Observations from morpho-tectonic analysis (Lourenço et al., 1998) and previous  
 368 campaign GPS surveys in the Central Group (Fernandes et al., 2006; Marques et al., 2013)  
 369 show evidence that the Eurasian-Nubian boundary in the Azores is diffuse. Our obser-  
 370 vations from CGPS data are in line with this assessment. The Eurasian-Nubian motion  
 371 in the Azores appears not to change gradually across the inter-plate deformation zone  
 372 but instead is more focused in some areas, namely in the central area of São Miguel Is-  
 373 land and between Faial-Pico ridge and Terceira Island. In particular, a narrow area in  
 374 the central part of São Miguel Island accommodates at least half of predicted regional  
 375 spreading. The existence of active plate spreading in São Miguel Island is suggested from  
 376 other studies using both campaign (Trota et al., 2006) and CGPS data (J. Okada et al.,  
 377 2015).

378 Our results show spatial variations of the differential motion along the Eurasian-  
 379 Nubian plate boundary in the Azores Plateau. The broader deformation zone in the Cen-  
 380 tral Group is consistent with volcanism distributed over a wider area, while in São Miguel  
 381 Island, the deformation is more focused. Seismic activity is also focused in some areas  
 382 of the Eurasian-Nubian boundary (see Figure 1), with stronger earthquakes more con-  
 383 centrated in rift basins between the islands and in the central area of São Miguel Island.  
 384 From 2002 to 2010, the central area of São Miguel Island has experienced a higher seis-  
 385 mic activity than in the previous decades, mainly as swarms with events of small mag-  
 386 nitude (Silva et al., 2012).

387 There is evidence of low degrees of partial melting beneath the thick lithosphere  
 388 caused by a mantle anomaly centered under the Central Group (Moreira et al., 1999; Gente  
 389 et al., 2003; Yang et al., 2006). The existence of deep processes in the Central Group is  
 390 also suggested from the large locking depth of our preferred model dislocation in the area  
 391 (see Table 2) and the deep earthquake activity (see Figure 2B).

392 Analysis of geochemical data indicates that focused magmatism occurs along the  
 393 Terceira Rift below volcanic systems (Haase & Beier, 2003; Beier et al., 2008; Storch et  
 394 al., 2020). The existence of shallow processes in São Miguel Island is inferred from the  
 395 shallow locking depth of our modeled dislocation for the island (see Table 2) and the shal-  
 396 low earthquake activity (see Figure 3B). The shallow processes may weaken the crust  
 397 and cause strain localization. Strain focusing in the central area of the island may re-  
 398 late to the episodic intrusions at Fogo during volcano unrests.

399 The high temporal resolution of the CGPS data allows calculating velocities with  
 400 high precision and performing an inversion of the data using simple analytical models.  
 401 On the other hand, the low spatial resolution and poor distribution of CGPS stations  
 402 are limitations to the modeling. There is no geodetic data from large submarine areas,  
 403 and some islands have no CGPS stations or only a single station. In particular, our pref-  
 404 erence for CG1 model for the Central Group is constrained by the higher number of CGPS  
 405 stations located in Terceira, São Jorge, Faial and Pico islands, comparing with the Gra-  
 406 ciosa Island area.

407 The spatial variation of the crustal deformation and the seismicity distribution sug-  
 408 gest partitioning of strain release, in rift basins with tectonic earthquakes and on the is-  
 409 lands with volcano unrests. The spreading in the Eurasian-Nubian plate boundary in  
 410 the Azores follows patterns similar to other ultraslow mid-ocean ridges (Sibrant et al.,  
 411 2015; Storch et al., 2020). The ultra-slow spreading axes of the Gakkel Ridge and the  
 412 South Indian Ridge comprise segments showing amagmatic extension and segments with  
 413 magmatic extension (Cochran, 2008; Cannat et al., 2019).

414 We infer that some submarine areas of the Eurasian-Nubian plate boundary in the  
 415 Azores are presently subject to rifting, contributing to the remaining predicted plate spread-  
 416 ing not detected with our observations, such as the Povoação basin to the east of São  
 417 Miguel Island and the Hirondele basin between São Miguel and Terceira islands.

418 Previous campaign GPS surveys show evidence of continuous subsidence of Ter-  
 419 ceira Island (Miranda et al., 2012; Marques et al., 2015). The previous surveys show hor-  
 420 izontal residual velocities compatible with a deflation in the center of the island, but no  
 421 confirmation from the vertical component was possible. The horizontal velocities of Ter-  
 422 ceira stations from this study show a deviation towards the center of the island, which  
 423 agrees with a deflation source located in that area. The higher subsidence rate found in  
 424 TERC station in the central part of Terceira confirms the existence of deflation in the  
 425 area. The extended period of deformation and modeling results suggests that the defla-  
 426 tion could be due to crystallization and degassing of a underlying magma body or de-  
 427 compression of an hydrothermal system in the center of the island. The deflation could  
 428 contribute to concentrated seismicity occurring in the center of the island.

429 The time-series of the stations located around Fogo volcano (BVF1, RCHA, RIB1,  
 430 PCNG, and VFDC), on São Miguel Island, show disturbances related to unrest activ-  
 431 ity, signaling the likely accumulation of volcanic fluids below the volcano.

## 432 6 Conclusions

433 The current analysis of CGPS data from the Azores shows the importance of es-  
 434 timating high precision velocities. The analysis of long time-series with removed estimated  
 435 noise is critical to measure accurately the ultra-slow spreading rate in the region. The  
 436 results show that Flores and Graciosa islands have displacements close to predicted North  
 437 American and Eurasian motions, respectively, while São Miguel, Terceira, São Jorge, Fa-  
 438 ial and Pico islands have displacements in between predicted Eurasian and Nubian mo-  
 439 tions. The spreading in the Eurasian-Nubian plate boundary in the Azores occurs in a  
 440 wide area between the Mid-Atlantic Ridge and southeast of São Miguel Island. The inter-  
 441 plate motion does not change gradually across the boundary but is instead focused in

442 some areas, including the central area of São Miguel Island and between Faial-Pico ridge  
 443 and Terceira Island. Modeling, using a freely sliding dislocation below a locking depth,  
 444 in a uniform elastic half-space, predict a deep motion in the range of 2.4-2.7 mm yr<sup>-1</sup> di-  
 445 rected N(76.5-78.8)°E located in the Central Group and São Miguel Island. This mo-  
 446 tion account for more than half predicted Eurasian-Nubian relative plate motion. The  
 447 results suggest that spreading in the Central Group is dominated by deep processes while  
 448 in São Miguel is dominated by shallow processes. Transient deformation occurs at Fogo  
 449 volcano, São Miguel Island, due to unrest activity, and local subsidence occurs in Ter-  
 450 ceira Island explained by a continuous deflation source centered in the island.

#### 451 **Acknowledgments**

452 João D’Araújo is supported by a Ph.D. grant co-financed by the FEDER FSE program  
 453 (ACORES-10-5369-FSE-000002), supported by the Science and Technology Regional Fund,  
 454 the Azores Regional Government, and the European Union. The work also benefits from  
 455 the Azores Regional Service of Civil Defence (SRPCBA) support for the installation and  
 456 maintenance of CGPS stations. We express our gratitude to the REPRAA agency and  
 457 Marlene Antunes for sharing the CGPS data and all at CIVISA involved in installing,  
 458 maintaining, and running the CGPS and seismic networks and analyzing the seismic events.  
 459 We also thank the contribution from Benedikt Ófeigsson in the review of the time-series  
 460 analysis on the scope of the EUROVOLC project. The figures in this manuscript were  
 461 produced using the Generic Mapping Tools (Wessel et al., 2013). The GPS and seismic  
 462 data are available at Dryad via [https://datadryad.org/stash/share/VyqRrN2Dez5GPoWkds4d3p1uD2GE](https://datadryad.org/stash/share/VyqRrN2Dez5GPoWkds4d3p1uD2GE_yfpdpdrDoJ.ReQ)  
 463 [\\_yfpdpdrDoJ.ReQ](https://datadryad.org/stash/share/VyqRrN2Dez5GPoWkds4d3p1uD2GE_yfpdpdrDoJ.ReQ) with private status for peer review purposes (D’Araújo et al., 2021).

#### 464 **References**

- 465 Altamimi, Z., Métivier, L., & Collilieux, X. (2012). Itrf2008 plate motion model.  
 466 *Journal of Geophysical Research: Solid Earth*, *117*(B7).
- 467 Argus, D. F., Gordon, R. G., Heflin, M. B., Ma, C., Eanes, R. J., Willis, P., ...  
 468 Owen, S. E. (2010). The angular velocities of the plates and the velocity of  
 469 earth’s centre from space geodesy. *Geophysical Journal International*, *180*(3),  
 470 913–960.
- 471 Árnadóttir, T., Jiang, W., Feigl, K. L., Geirsson, H., & Sturkell, E. (2006). Kine-  
 472 matic models of plate boundary deformation in southwest iceland derived from  
 473 gps observations. *Journal of Geophysical Research: Solid Earth*, *111*(B7).
- 474 Battaglia, M., Cervelli, P. F., & Murray, J. R. (2013). dmodels: A matlab soft-  
 475 ware package for modeling crustal deformation near active faults and volcanic  
 476 centers. *Journal of Volcanology and Geothermal Research*, *254*, 1–4.
- 477 Becker, J., Sandwell, D., Smith, W., Braud, J., Binder, B., Depner, J., ... others  
 478 (2009). Global bathymetry and elevation data at 30 arc seconds resolution:  
 479 Srtm30\_plus. *Marine Geodesy*, *32*(4), 355–371.
- 480 Beier, C., Haase, K. M., Abouchami, W., Krienitz, M.-S., & Hauff, F. (2008).  
 481 Magma genesis by rifting of oceanic lithosphere above anomalous mantle:  
 482 Terceira rift, azores. *Geochemistry, Geophysics, Geosystems*, *9*(12).
- 483 Böhm, J., Niell, A., Tregoning, P., & Schuh, H. (2006). Global mapping function  
 484 (gmf): A new empirical mapping function based on numerical weather model  
 485 data. *Geophysical Research Letters*, *33*(7).
- 486 Cannat, M., Sauter, D., Lavier, L., Bickert, M., Momoh, E., & Leroy, S. (2019). On  
 487 spreading modes and magma supply at slow and ultraslow mid-ocean ridges.  
 488 *Earth and Planetary Science Letters*, *519*, 223–233.
- 489 Carmo, R., Madeira, J., Hipólito, A., & Ferreira, T. (2014). Paleoseismological  
 490 evidence for historical surface faulting in são miguel island (azores). *Annals of*  
 491 *Geophysics*, *56*(6).
- 492 Cochran, J. R. (2008). Seamount volcanism along the gakkel ridge, arctic ocean.

- 493 *Geophysical Journal International*, 174(3), 1153–1173.
- 494 Dach, R., & Walser, P. (2015). Bernese gnss software version 5.2 [Computer software  
495 manual]. Citeseer.
- 496 D’Araújo, J., Sigmundsson, F., Okada, J., Ferreira, T., Lorenzo, M., & Silva,  
497 R. (2021). Plate boundary deformation at the azores triple junction de-  
498 termined from continuous gps geodetic measurements, 2000-2017. *Dryad*.  
499 <https://doi.org/10.5061/dryad.31zcrjdm3>.
- 500 DeMets, C., Gordon, R. G., & Argus, D. F. (2010). Geologically current plate mo-  
501 tions. *Geophysical Journal International*, 181(1), 1–80.
- 502 Drouin, V., Heki, K., Sigmundsson, F., Hreinsdóttir, S., & Ófeiggsson, B. G. (2016).  
503 Constraints on seasonal load variations and regional rigidity from continuous  
504 gps measurements in iceland, 1997–2014. *Geophysical Journal International*,  
505 205(3), 1843–1858.
- 506 Escartin, J., Cannat, M., Pouliquen, G., Rabain, A., & Lin, J. (2001). Crustal  
507 thickness of v-shaped ridges south of the azores: Interaction of the mid-atlantic  
508 ridge (36–39 n) and the azores hot spot. *Journal of Geophysical Research:*  
509 *Solid Earth*, 106(B10), 21719–21735.
- 510 Fernandes, R., Bastos, L., Miranda, J., Lourenço, N., Ambrosius, B., Noomen, R., &  
511 Simons, W. (2006). Defining the plate boundaries in the azores region. *Journal*  
512 *of Volcanology and Geothermal Research*, 156(1-2), 1–9.
- 513 Gaspar, J., Queiroz, G., Ferreira, T., Medeiros, A., Goulart, C., & Medeiros, J.  
514 (2015). Earthquakes and volcanic eruptions in the azores region: geodynamic  
515 implications from major historical events and instrumental seismicity. *Geologi-*  
516 *cal Society, London, Memoirs*, 44(1), 33–49.
- 517 Geirsson, H., Árnadóttir, T., Völksen, C., Jiang, W., Sturkell, E., Villemin, T., ...  
518 Stefánsson, R. (2006). Current plate movements across the mid-atlantic ridge  
519 determined from 5 years of continuous gps measurements in iceland. *Journal of*  
520 *Geophysical Research: Solid Earth*, 111(B9).
- 521 Gente, P., Dymont, J., Maia, M., & Goslin, J. (2003). Interaction between the  
522 mid-atlantic ridge and the azores hot spot during the last 85 myr: Emplace-  
523 ment and rifting of the hot spot-derived plateaus. *Geochemistry, Geophysics,*  
524 *Geosystems*, 4(10).
- 525 Haase, K. M., & Beier, C. (2003). Tectonic control of ocean island basalt sources on  
526 são miguel, azores? *Geophysical Research Letters*, 30(16).
- 527 Jónsson, S., Alves, M. M., & Sigmundsson, F. (1999). Low rates of deformation of  
528 the furnas and fogo volcanoes, são miguel, azores, observed with the global po-  
529 sitioning system, 1993–1997. *Journal of Volcanology and Geothermal Research*,  
530 92(1-2), 83–94.
- 531 Keiding, M., Árnadóttir, T., Sturkell, E., Geirsson, H., & Lund, B. (2008). Strain  
532 accumulation along an oblique plate boundary: the reykjanes peninsula, south-  
533 west iceland. *Geophysical Journal International*, 172(2), 861–872.
- 534 Lourenço, N., Miranda, J., Luis, J., Ribeiro, A., Victor, L. M., Madeira, J., & Need-  
535 ham, H. (1998). Morpho-tectonic analysis of the azores volcanic plateau from  
536 a new bathymetric compilation of the area. *Marine Geophysical Researches*,  
537 20(3), 141–156.
- 538 Luis, J. F., Miranda, J., Galdeano, A., Patriat, P., Rossignol, J., & Victor, L. M.  
539 (1994). The azores triple junction evolution since 10 ma from an aeromag-  
540 netic survey of the mid-atlantic ridge. *Earth and Planetary Science Letters*,  
541 125(1-4), 439–459.
- 542 Lyard, F., Lefevre, F., Letellier, T., & Francis, O. (2006). Modelling the global  
543 ocean tides: modern insights from fes2004. *Ocean dynamics*, 56(5-6), 394–415.
- 544 Machado, F. (1959). Submarine pits of the azores plateau. *Bulletin of Volcanology*,  
545 21(1), 109–116.
- 546 Madeira, J., da Silveira, A. B., Hipólito, A., & Carmo, R. (2015). Active tectonics  
547 in the central and eastern azores islands along the eurasia–nubia boundary: a

- 548 review. *Geological Society, London, Memoirs*, 44(1), 15–32.
- 549 Marques, F., Catalão, J., DeMets, C., Costa, A., & Hildenbrand, A. (2013). Gps  
550 and tectonic evidence for a diffuse plate boundary at the azores triple junction.  
551 *Earth and Planetary Science Letters*, 381, 177–187.
- 552 Marques, F., Catalão, J., Hildenbrand, A., & Madureira, P. (2015). Ground mo-  
553 tion and tectonics in the terceira island: Tectonomagmatic interactions in an  
554 oceanic rift (terceira rift, azores triple junction). *Tectonophysics*, 651, 19–34.
- 555 Matias, L., Dias, N., Morais, I., Vales, D., Carrilho, F., Madeira, J., ... Silveira,  
556 A. (2007). The 9th of july 1998 faial island (azores, north atlantic) seismic  
557 sequence. *Journal of Seismology*, 11(3), 275–298.
- 558 Mendes, V., Madeira, J., da Silveira, A. B., Trota, A., Elosegui, P., & Pagarete, J.  
559 (2013). Present-day deformation in são jorge island, azores, from episodic gps  
560 measurements (2001–2011). *Advances in Space Research*, 51(8), 1581–1592.
- 561 Miranda, J., Navarro, A., Catalão, J., & Fernandes, R. (2012). Surface displace-  
562 ment field at terceira island deduced from repeated gps measurements. *Journal*  
563 *of Volcanology and Geothermal Research*, 217, 1–7.
- 564 Mogi, K. (1958). Relations between the eruptions of various volcanoes and the defor-  
565 mations of the ground surfaces around them. *Earthq Res Inst*, 36, 99–134.
- 566 Moreira, M., Doucelance, R., Kurz, M. D., Dupré, B., & Allègre, C. J. (1999). He-  
567 lium and lead isotope geochemistry of the azores archipelago. *Earth and Plane-*  
568 *tary Science Letters*, 169(1-2), 189–205.
- 569 Okada, J., Sigmundsson, F., Ófeigsson, B. G., Ferreira, T. J., & Rodrigues, R. M.  
570 (2015). Tectonic and volcanic deformation at são miguel island, azores, ob-  
571 served by continuous gps analysis 2008–13. *Geological Society, London, Mem-*  
572 *oirs*, 44(1), 239–256.
- 573 Okada, Y. (1985). Surface deformation due to shear and tensile faults in a half-  
574 space. *Bulletin of the Seismological Society of America*, 75(4), 1135–1154.
- 575 REPRAA. (2021). *Rede de estações permanentes da região autónoma dos açores*.  
576 <https://repra.azores.gov.pt/>. (Accessed: 2021-07-02)
- 577 Schmid, R., Dach, R., Collilieux, X., Jäggi, A., Schmitz, M., & Dilssner, F. (2016).  
578 Absolute igs antenna phase center model igs08.atx: status and potential im-  
579 provements. *Journal of Geodesy*, 90(4), 343–364.
- 580 Searle, R. (1980). Tectonic pattern of the azores spreading centre and triple junc-  
581 tion. *Earth and Planetary Science Letters*, 51(2), 415–434.
- 582 Sibrant, A., Hildenbrand, A., Marques, F., Weiss, B., Boulesteix, T., Hübscher, C.,  
583 ... Catalão, J. (2015). Morpho-structural evolution of a volcanic island de-  
584 veloped inside an active oceanic rift: S. miguel island (terceira rift, azores).  
585 *Journal of Volcanology and Geothermal Research*, 301, 90–106.
- 586 Silva, R., Havskov, J., Bean, C., & Wallenstein, N. (2012). Seismic swarms, fault  
587 plane solutions, and stress tensors for são miguel island central region (azores).  
588 *Journal of Seismology*, 16(3), 389–407.
- 589 Spieker, K., Rondenay, S., Ramalho, R., Thomas, C., & Helffrich, G. (2018). Con-  
590 straints on the structure of the crust and lithosphere beneath the azores is-  
591 lands from teleseismic receiver functions. *Geophysical Journal International*,  
592 213(2), 824–835.
- 593 Storch, B., Haase, K., Romer, R., Beier, C., & Koppers, A. (2020). Rifting of the  
594 oceanic azores plateau with episodic volcanic activity. *Scientific reports*, 10(1),  
595 1–12.
- 596 Susnik, A., Dach, R., Villiger, A., Maier, A., Arnold, D., Schaer, S., & Jäggi, A.  
597 (2016). *Code reprocessing product series*. Astronomical Institute, University of  
598 Bern.
- 599 Trota, A. (2008). Crustal deformation studies in s. miguel and terceira islands  
600 (azores). volcanic unrest evaluation in fogo/congro area (s. miguel). *PhD*  
601 *Thesis in Geology. Universidade dos Açores (281p)*.
- 602 Trota, A., Houlié, N., Briole, P., Gaspar, J., Sigmundsson, F., & Feigl, K. (2006).

- 603 Deformation studies at furnas and sete cidades volcanoes (são miguel island,  
604 azores). velocities and further investigations. *Geophysical Journal Interna-*  
605 *tional*, 166(2), 952–956.
- 606 Wessel, P., Smith, W. H., Scharroo, R., Luis, J., & Wobbe, F. (2013). Generic map-  
607 ping tools: improved version released. *Eos, Transactions American Geophysical*  
608 *Union*, 94(45), 409–410.
- 609 Yang, T., Shen, Y., van der Lee, S., Solomon, S. C., & Hung, S.-H. (2006). Up-  
610 per mantle structure beneath the azores hotspot from finite-frequency seismic  
611 tomography. *Earth and Planetary Science Letters*, 250(1-2), 11–26.

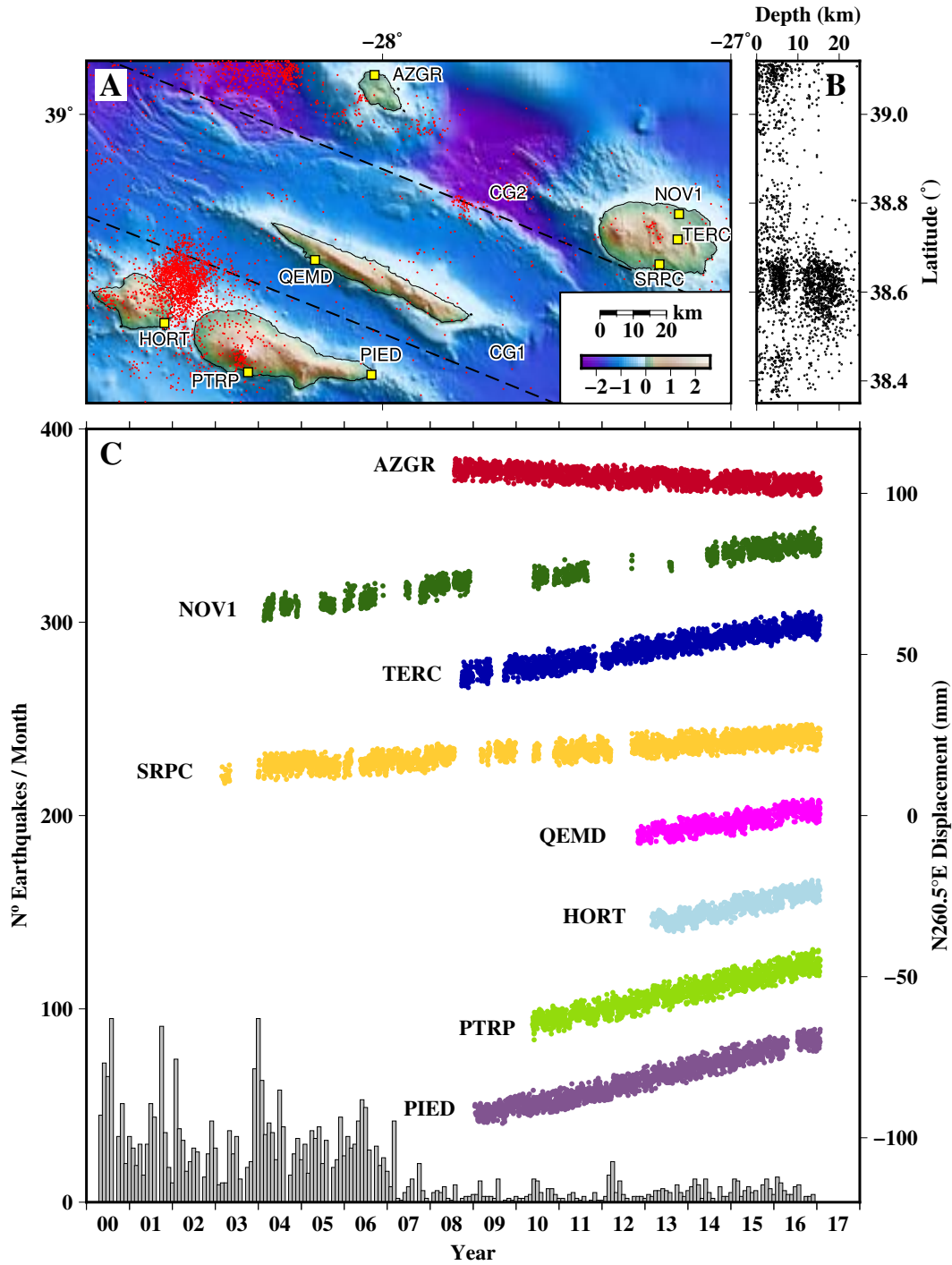


**Figure 2.** A - Location of the CGPS stations AZGR, NOV1, TERC, SRPC, QEMD, HORT, PTRP and PIED located in the Central Group. Red circles are recorded earthquakes ( $M_C \geq 2$ ). Dashed lines are the profiles CG1 and CG2 modeled in this study for the area. B - Time-series of the CGPS stations movement relative to predicted ITRF2008 Eurasian motion (Altamimi et al., 2012), transformed onto the direction away from predicted Eurasian motion ( $N260.5^\circ E$ ). The times-series are shifted from top to bottom to display the CGPS stations movement from the north (AZGR) to the south (PIED). The vertical gray bars are the monthly number of earthquakes in the area ( $M_C \geq 2$ ).

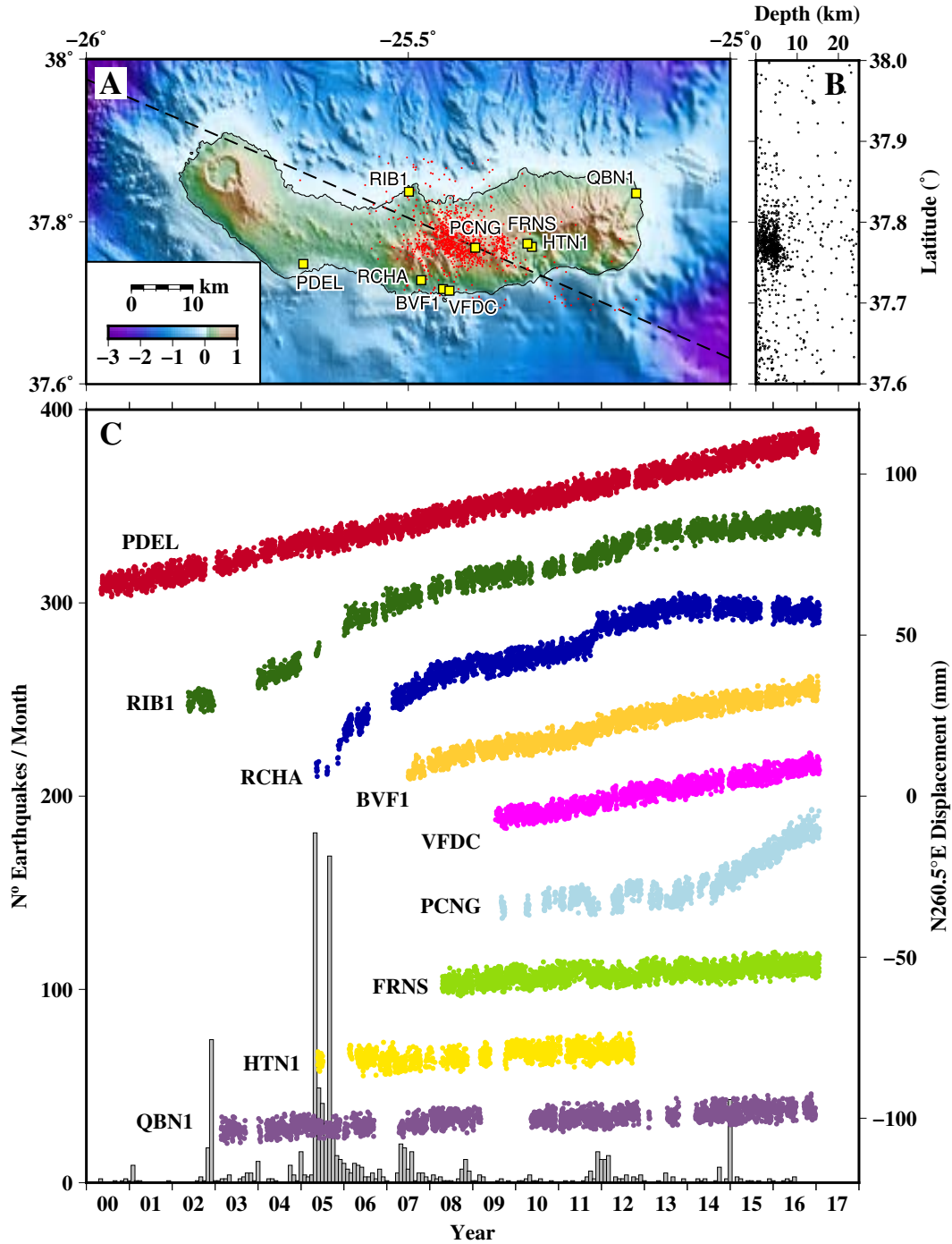


**Figure 3.** A - Location of the CGPS stations PDEL, RIB1, RCHA, BVF1, VFDC, PCNG, FRNS, HTN1 and QBN1 located in São Miguel Island. Red circles are recorded earthquakes ( $M_C \geq 2$ ), concentrated between Fogo and Furnas volcanoes. Dashed line is the profile SM1 modeled in this study for the area. B - Time-series of the CGPS stations movement relative to predicted ITRF2008 Eurasian motion (Altamimi et al., 2012), transformed onto the direction away from predicted Eurasian motion (N260.5°E). The times-series are shifted from top to bottom to display the CGPS stations movement from the west (PDEL) to the east (QBN1). The vertical gray bars are the monthly number of earthquakes in the area ( $M_C \geq 2$ ).

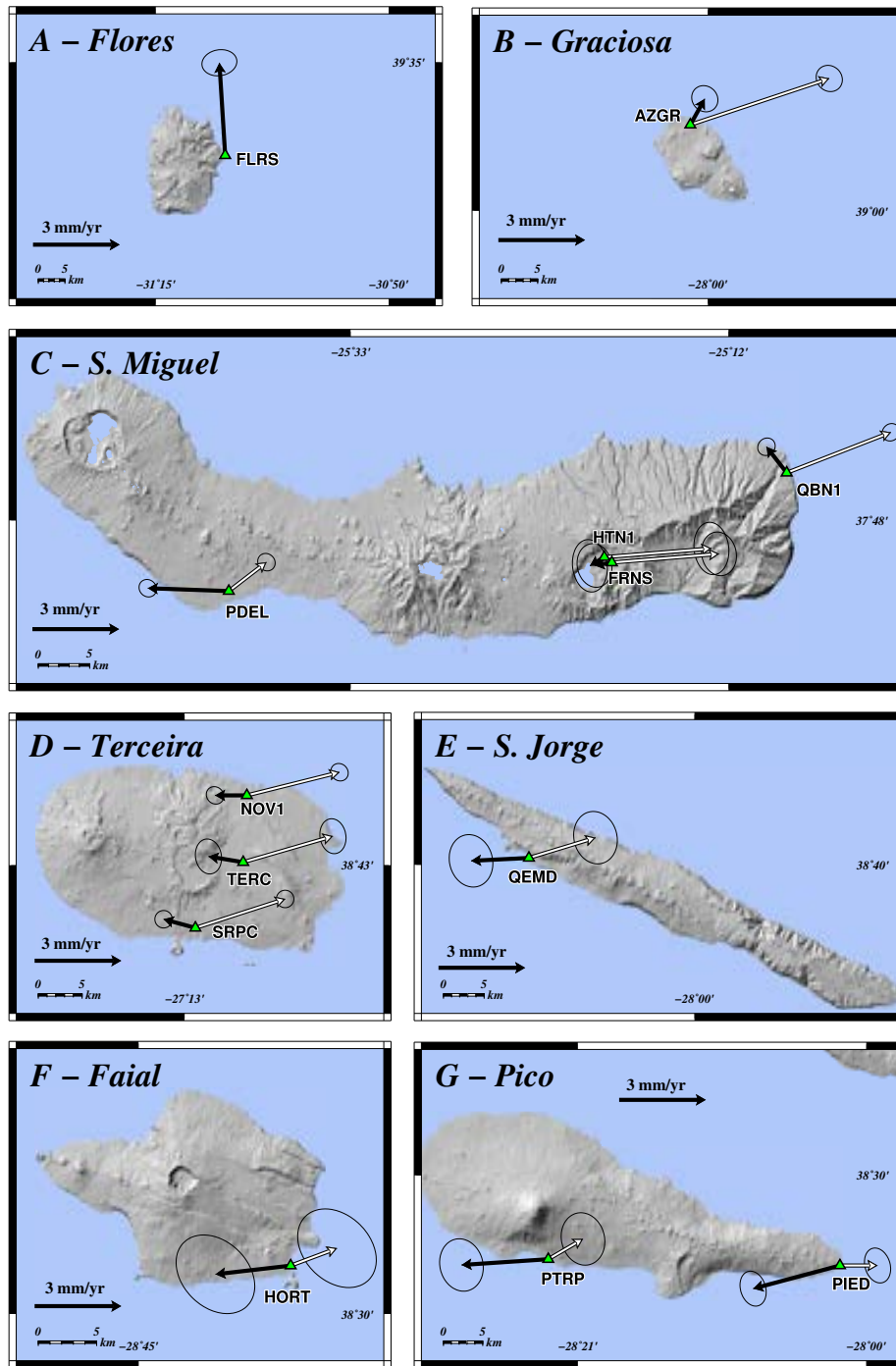


**Figure 4.** Horizontal velocities of CGPS stations located on Flores (A), Graciosa (B), São Miguel (C), Terceira (D), São Jorge (E), Faial (F) and Pico (G). In figure A, the black arrow represent the velocity from Table 1 relative to predicted ITRF2008 North American motion. In figures from B to G, the black and white arrows represent the velocities from Table 1 relative to predicted ITRF2008 Eurasian and Nubian motions, respectively (Altamimi et al., 2012). The ellipses represent the  $1\sigma$  confidence level and the green triangles are the CGPS stations.

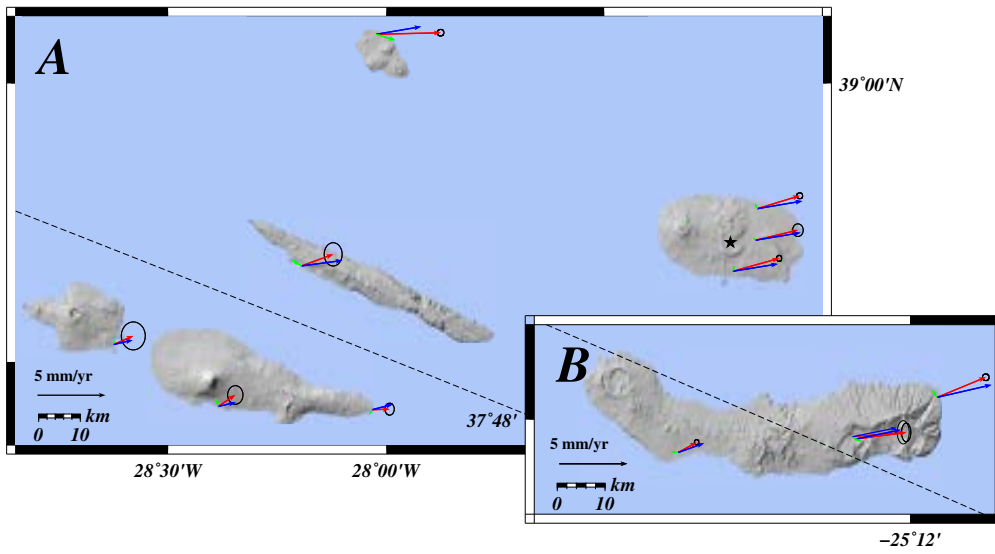


**Figure 5.** Results of kinematic plate boundary modeling of the horizontal velocities for Central Group (A) and São Miguel Island (B). The velocity arrows show observed corrected from Mogi source (blue,  $2\sigma$  confidence ellipses), predicted from data inversion using Okada dislocations (red), and residuals (green). The dislocations CG1 (A) and SM1 (B) are shown with dashed black lines. Mogi source is shown with black star (A).